Quantum Electronics **35** (5) 435–441 (2005)

FIBRE LASERS

PACS numbers: 42.55.Wd; 42.55.Ye; 42.60.Jf
DOI: 10.1070/QE2005v035n05ABEH003415

Raman fibre lasers based on heavily GeO_2-doped fibres

E.M. Dianov, I.A. Bufetov, V.M. Mashinsky, A.V. Shubin,
O.I. Medvedkov, A.E. Rakitin, M.A. Melkumov, V.F. Khopin, A.N. Gur'yanov

Abstract. **Amplification of radiation due to stimulated Raman scattering in an optical fibre with a heavily GeO_2-doped core and a fused silica cladding is studied. The applications of such fibres in Raman lasers are demonstrated. A Raman fibre laser emitting 10 W at a fibre length of only 3 m and Raman lasers emitting at 1.73, 1.85, 2.06, and 2.2 μm are fabricated for the first time.**

Keywords: *Raman fibre laser, GeO_2-doped optical fibre.*

1. Introduction

Fibre lasers based on fused silica emit radiation in a broad IR range from 0.9 to 2.1 μm (Fig. 1). Some spectral regions within this range are covered by radiation from rare-earth-ion-doped fibre lasers, while Raman fibre lasers emit in the region from 1.12 to 1.65 μm [1].

The extension of the emission range of fibre lasers to the longer-wavelength region would allow the fabrication of convenient radiation sources which could find applications for environment monitoring, in medicine, scientific studies, and other fields. This is impeded by the increase in the optical losses in silica fibres in the wavelength range above 2 μm.

In particular, when optical losses dominate in a fibre, the threshold power P_{th} of fibre lasers increases proportionally to the loss factor α_s ($P_{th} = \alpha_s/g_0$, where g_0 is the Raman gain in the fibre) [2]. Typical optical losses α_s of standard germanosilicate fibres (with a fused silica core doped with GeO_2 at a molar concentration of ~ 3 %) at a wavelength of 2.1 μm are about 100 dB km^{-1} for $g_0 < 3$ dB km^{-1} W^{-1}. Therefore, according to the lower bound, the threshold pump power for a Raman fibre laser based on standard fibres in this wavelength region is very high, amounting to $P_{th} \approx 30$ W.

E.M. Dianov, I.A. Bufetov, V.M. Mashinsky, A.V. Shubin, O.I. Medvedkov, A.E. Rakitin, M.A. Melkumov Fiber Optics Research Center, A.M. Prokhorov General Physics Institute, Russian Academy of Sciences, ul. Vavilova 38, 119991 Moscow, Russia; Tel.: (095) 132 82 56; Fax: (095) 135 81 39; e-mail: iabuf@fo.gpi.ru;
V.F. Khopin, A.N. Gur'yanov Institute of Chemistry of High-Purity Substances, Russian Academy of Sciences, ul. Tropinina 4, 603600 Nizhny Novgorod, Russia; Tel.: (831) 212 73 13; Fax: (831) 266 46 34; e-mail: vkhopin@mail.ru

Received 13 January 2005
Kvantovaya Elektronika **35** (5) 435–441 (2005)
Translated by M.N. Sapozhnikov

The threshold power can be decreased down to the acceptable level of ~ 1 W only by increasing the Raman gain and decreasing optical losses.

It is known that the fundamental minimum of optical losses in a GeO_2 glass lies in the region of 2 μm [3, 4] and is ~ 0.22 dB km^{-1}. Due to a great difference between the refractive indices of a fibre core and cladding ($\Delta n \sim 0.1$), optical fibres with a fused silica cladding and a core consisting mainly of GeO_2 (hereafter, GeO_2 fibres) have a small diameter of the mode field and, hence, should have a high Raman gain. The SRS cross section in a GeO_2 glass is approximately an order of magnitude higher than that in a silica glass [5], so that a high concentration of GeO_2 in the fibre core additionally enhances the Raman gain. Generally speaking, a small diameter of the mode field provides a high efficiency of various nonlinear effects. Thus, GeO_2 fibres are first of all of interest due to their comparatively low optical losses at 2 μm and their nonlinear properties.

Although the fabrication of single-mode GeO_2 fibres with low optical losses involves certain technological problems, by using MCVD technologies, we have managed to fabricate GeO_2 fibres with minimal optical losses 20–100 dB km^{-1} in the spectral range between 1.8 and 1.9 μm. This level of losses is substantially higher than the minimal possible level, but high Raman gains allow the use of these fibres as an amplifying medium. In addition, these fibres are sufficiently photosensitive for writing fibre Bragg gratings (FBGs) in them, which are used as laser mirrors [6].

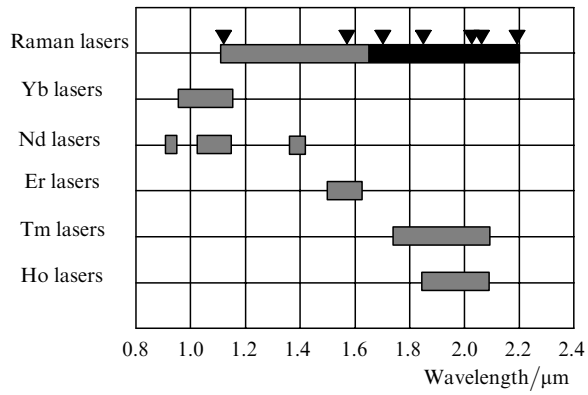

Figure 1. Emission regions of fibre lasers based on fused silica in the 0.9–2.2-μm range: dark rectangles are Raman GeO_2 fibre lasers; triangles indicate the wavelengths of Raman lasers fabricated in this work.

Thus, the use of GeO_2 fibres with a silica cladding in Raman fibre lasers considerably extended the emission range of these lasers up to 2.2 μm (Fig. 1).

2. Amplifying properties of a GeO_2 fibre

As an amplifying medium of a Raman fibre laser, we used a GeO_2 fibre with the cut off wavelength $\lambda_c = 1.42$ μm, a core diameter of 2 μm, and the 75 % molar content of GeO_2 in the fibre core. The distribution of the GeO_2 concentration was measured by the method of X-ray microanalysis with a JEOL JSM-5910LV scanning electron microscope and an Oxford Instruments INCA X-ray spectrometer. The fibre core section had the elliptic form (with the axial ratio 3 : 4). Despite a high content of germanium in the core, the minimal optical losses at 1.9 μm were 20 dB km^{-1}. In the wavelength region above 2 μm, optical losses in the GeO_2 fibre were lower than those in a standard SMF-28 telecommunication fibre, being ~30 dB km^{-1} at a wavelength of 2 μm. The zero-dispersion wavelength for the GeO_2 fibre was ~2.5 μm, which is important for the suppression of four-wave mixing in the wavelength region up to ~2.4 μm. The parameters of the fibre are described in more detail in [2, 6].

In all Raman fibre lasers, GeO_2 fibres of length 3 – 60 m were used as an amplifying element. FBGs were written in all cases directly in these fibres, which excluded the appearance of lumped losses in optical resonators in fibre splices. The spectral width of all FBGs was ~1 nm. Raman fibre lasers were spliced with single-mode cw pump sources such as a 1.07-μm Yb-doped fibre laser with a multielement first cladding (known also as a GTWave fibre) [7], a 1.47-μm two-stage Raman phosphosilicate fibre laser [8], and a 1.608-μm Er/Yb-doped fibre laser [7].

By using these pump lasers, the Raman gain was measured at wavelengths 1.12, 1.57, and 1.72 μm by the method based on measuring the lasing threshold of a Raman fibre laser [9]. The following results were obtained: the maximum Raman gain at a wavelength of 1.12 μm upon pumping at 1.07 μm was $g_0(1.12/1.07) = 300$ dB km^{-1} W^{-1}, $g_0(1.57/1.47) = 112$ dB km^{-1} W^{-1}, $g_0(1.73/1.61) = 59$ dB km^{-1} W^{-1} (Fig. 2). The maximum Raman gain in GeO_2 fibres corresponded to the frequency shift ≈ 427 cm^{-1}. As follows from these data, the Raman gain drastically decreases with increase wavelength.

The Raman gain at other wavelengths was calculated taking into account the field distribution in a fibre with the specified refractive-index profile and GeO_2 concentration distribution in the fibre core [10]. It was assumed that the Raman gain in the fibre decreases inversely proportionally to the wavelength [11]. Figure 2 shows the Raman gain $g_0(\lambda)$ calculated for three maximum concentrations of GeO_2 in the fibre core for the same refractive-index profile. The molar concentration of GeO_2 equal to 75 % corresponds to that in a preform (before fibre drawing); the concentration 52 % corresponds to the difference Δn at which the calculated diameter of the fundamental-mode field of the fibre coincides with its value measured by the far-field method, and only at the concentration 40 % the best agreement between the calculation and experimental data is achieved. The discrepancy between the calculations and experiment is observed in all cases (Fig. 2), the experimental Raman gain decreasing with the wavelength more rapidly than the calculated gain.

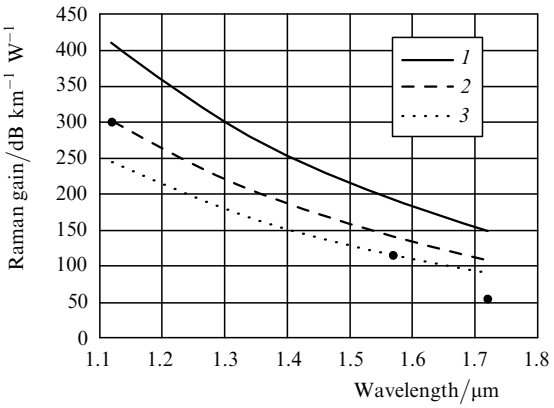

Figure 2. Spectral dependences of the Raman gain in a fibre with a heavily GeO_2-doped core for different molar concentrations of GeO_2: (*1*, *2*, *3*) are curves calculated for the maximum GeO_2 concentration equal to 75 %, 52 %, and 40 %, respectively. Points are experimental results obtained at the GeO_2 concentration equal to 75 %.

The error in calculations of $g_0(\lambda)$ can be caused by the fact that the data on the refractive-index profile in the fibre were mainly obtained by measuring the GeO_2 concentration distribution over the preform cross section because the refractive index was measured with specialised York Technology P-102 instruments, which were not intended for measuring such large values of Δn (~0.1). However, the variation of the refractive-index profile within the possible measurement error also does not provide agreement between experimental and calculated Raman gains. Therefore, further studies are needed to elucidate the reason for this discrepancy.

3. 1.12-μm one-stage Raman GeO_2 fibre laser

Optical losses in the GeO_2 fibre at a wavelength of ~1.1 μm are high, amounting to ~120 dB km^{-1}. However, a high Raman gain in this spectral region well compensates this drawback, which made it possible to fabricate a cw Raman laser based on a very short fibre. Indeed, the quality parameter $P_F = [(\alpha_p/g_0)^{1/2} + (\alpha_1/g_0)^{1/2}]^2$ [12] (α_p and α_1 are optical losses in the fibre at the pump wavelength and the first Stokes component, respectively) of the GeO_2 fibre used in one-stage Raman laser is ~1.6 W at wavelengths 1.07 and 1.12 μm. This value corresponds approximately to P_F for optical fibres employed in highly efficient Raman fibre lasers [12].

We calculated and fabricated a 1.12-μm Raman GeO_2 fibre laser pumped by a 1.07-μm Yb-doped fibre laser. The optimal length of the active fibre was only 3 m. The scheme of the laser is presented in Fig. 3.

Figure 4 shows the dependence of the output power of this laser on the pump power. The maximum output power achieved 10 W, being limited only by the appearance of lasing at the second Stokes component in the resonator formed by the end-faces of the GeO_2 and ytterbium fibres. For comparison, we present here a similar dependence for a Raman fibre laser based on a fibre of length 20 m, which was used for measuring the Raman gain.

Due to the broadening of the emission spectrum of the Raman laser, a part of its radiation emerged not from the FBG output coupler (OC) but through a highly reflecting (HR) grating of the 1.07-μm Yb laser at the other end of the

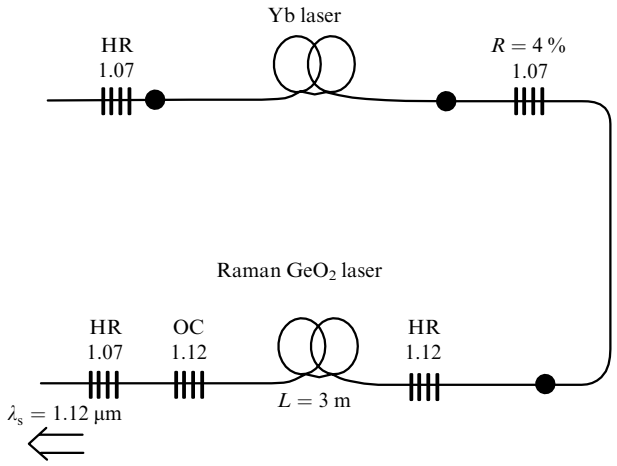

Figure 3. Scheme of the 1.12-μm Raman GeO_2 fibre laser with the fibre length 3 m. Over FBGs are shown resonance wavelengths (in μm) and reflectivities (HR corresponds to the reflectivity close to 100 %); OC is the output grating; dark circles show splices.

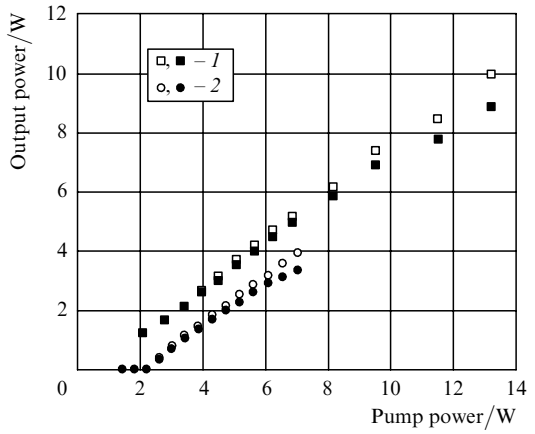

Figure 4. Dependences of the output power of the 1.12-μm one-stage Raman laser on the 1.07-μm pump power for the fibre length equal to 3 m (*1*) and 20 m without the output 1.12-μm FBG (OC in Fig. 3) (*2*) for measuring g_0. Dark circles and squares correspond to the output power of the laser; open circles and squares correspond to the total power of the Stokes component at the laser output and radiation transmitted through the 1.07-μm HR grating of the Yb laser.

fibre scheme. The dark circles and squares in Fig. 4 correspond to the Raman laser output power at the OC, while open circles and squares correspond to the total Stokes component power behind the OC and the 1.07-μm HR grating of the Yb laser.

The efficiency of the laser with the fibre length of 3 m was 70 %, demonstrating the potential possibilities of using heavily GeO_2-doped fibres as active fibres in Raman lasers. A small length of active fibres, high values of Δn and, hence, low bending losses allow one to hope to develop miniature Raman fibre lasers of size as small as a few centimetres.

4. Raman GeO_2 fibre lasers pumped at 1.47 μm

The spectral dependence of optical losses in GeO_2 fibres shows that efficient Raman fibre lasers emitting at $\sim$2 μm can be fabricated. However, the frequency shift corresponding to the maximum Raman gain in GeO_2 fibres is too small for obtaining lasing at 2 μm upon pumping by the 1.07-μm radiation because this can be achieve only by using at least a ten-stage Raman laser. For this reason, we used in our experiments pumping at longer wavelengths.

In the scheme presented in Fig. 5, the Raman GeO_2 fibre laser was pumped by a two-stage Raman phosphosilicate fibre laser, which in turn was pumped by a 1.06-μm Yb-doped fibre laser [8]. The GeO_2 fibre end perpendicular to the geometrical axis played the role of the output mirror with a reflectivity of 3.5 %. An FBG returning to the resonator the pump radiation that has not been absorbed during one round trip was absent. In this case, Raman lasing occurred at the wavelength $\lambda_s = 1571$ nm. The lasing power achieved 3.5 W for the efficiency equal to 60 %. Figure 6 shows the dependence of the output power on the 1472-nm pump power and the emission spectrum of the laser. Note that the spectrum exhibits apart from the main peak at $\lambda_s = 1571$ nm its satellites at $\lambda_2 = 1556$ nm and $\lambda_3 = 1584$ nm, corresponding to the frequency shift $\sim$56 cm^{-1}. The side peaks are probably caused by four-photon mixing according to the scheme $2h\nu_1 \rightarrow h\nu_2 + h\nu_3$, where ν_i is the frequency corresponding to the wavelength λ_i. The phase-matching conditions are fulfilled in this case due to the difference between the propagation constants of modes with different polarisations propagating in the fibre with birefringence caused by the elliptic shape of the fibre core. This circumstance is confirmed by the fact that the satellites at λ_2 and λ_3 are polarised in mutually perpendicular planes [13].

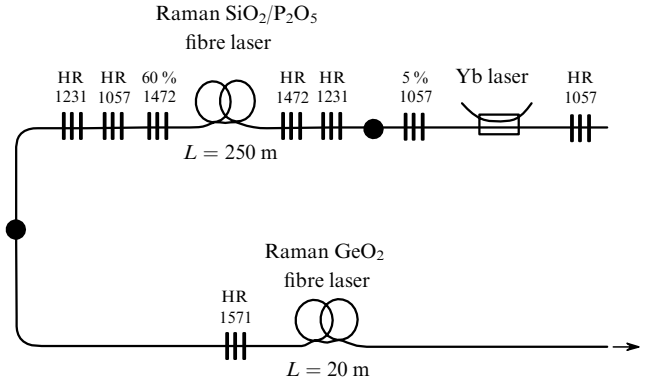

Figure 5. Scheme of the 1571-nm Raman fibre laser pumped by the two-stage Raman phosphosilicate fibre laser. Over FBGs are shown the resonance wavelengths in nanometres and reflectivities (HR corresponds to the reflectivity close to 100 %).

By increasing the number of stages in the Raman GeO_2 fibre laser pumped at 1.47 μm, lasing at 2 μm can be achieved. We used for this purpose the four-stage Raman GeO_2 fibre laser based on the fibre of length 18 m. In this case, the resonance wavelengths of FBGs with the frequency shift somewhat greater than 427 cm^{-1} were selected to achieve lasing in the region above 2 μm: $\lambda_p = 1472.5$ nm, $\lambda_{s1} = 1574.5$ nm, $\lambda_{s2} = 1695$ nm $\lambda_{s3} = 1853$ nm, and $\lambda_{s4} = 2062$ nm. The transmission coefficient of the output grating was 50 %.

Pumping was performed by a two-stage Raman phosphosilicate fibre laser [8]. The maximum 1472-nm pump power was 6.25 W. Figure 7 shows the scheme of the laser.

Figure 8a shows the emission spectrum of this Raman laser. The laser was pumped by 3.9 W at 1472 nm. The

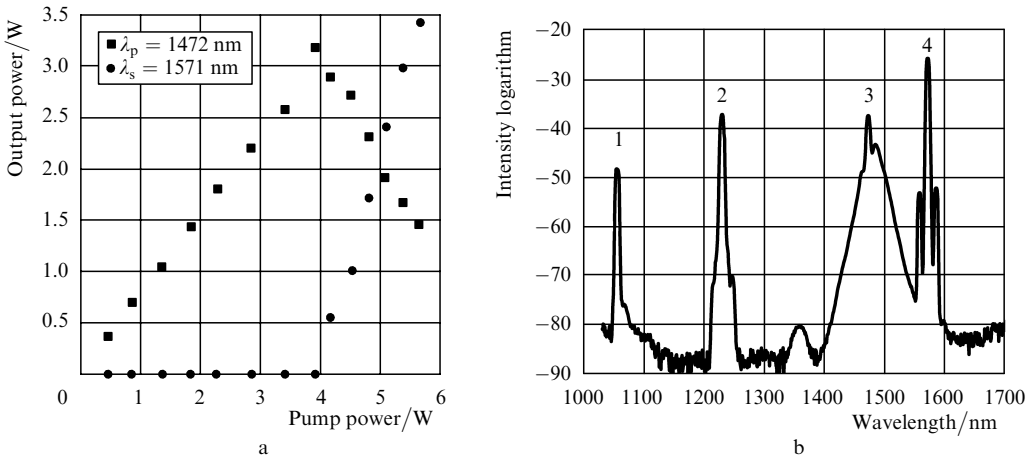

Figure 6. Dependences of the output power of the 1571-nm Raman laser based on the GeO_2 fibre of length 20 m on the 1472-nm pump power (a) and the emission spectrum of the composite Raman laser (b); peak 1: the unabsorbed 1057-nm pump radiation from the Yb fibre laser; peak 2: the 1231-nm radiation of the first stage of the Raman phosphosilicate fibre laser; peak 3: the 1472-nm radiation of the second stage of the Raman phosphosilicate fibre laser used to pump the one-stage Raman GeO_2 fibre laser; and peak 4: the 1571-nm radiation of the Raman GeO_2 fibre laser.

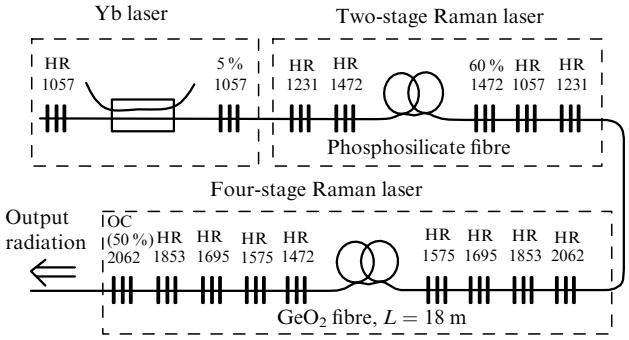

Figure 7. Scheme of the 2062-nm four-stage Raman fibre laser.

spectrum was recorded in the spectral range below 2 μm using an MDR-4 monochromator in the second diffraction order and in the spectral range above 2 μm in the first diffraction order. Peak 1 at 1057 nm corresponds to the unabsorbed radiation of the Yb fibre laser used for pumping the Raman phosphosilicate fibre laser. Peaks 2 and 3 correspond to the first and second Stokes components of the Raman phosphosilicate fibre laser. The first three Stokes components of the Raman germanate fibre laser are denoted by the numbers 4, 5, and 6, respectively. The fourth Stokes component of this laser (peak 8 at $\lambda_{s4} = 2062$ nm) was recorded in the first diffraction order near peak 1 at 1057 nm. Weak peak 7 at 2017 nm probably corresponds to the maximum of the Raman gain of peak 6 (the third Stokes component at $\lambda_{s3} = 1853$ nm in the GeO_2 fibre): here, Raman lasing is observed despite the absence of a high-Q optical resonator at this wavelength.

It follows from Fig. 8b that, as in the case of one-stage Raman GeO_2 fibre laser ($\lambda_{s1} = 1571$ nm), parametric amplification takes place in the region of the first Stokes component (four-photon mixing due to birefringence caused by the elliptic shape of the fibre core). In this case, the frequency shift differs somewhat from that observed in the one-stage Raman laser and is approximately 53 cm^{-1}.

Figure 9 shows the dependences of the power of different components of the output radiation of the four-stage Raman laser on the pump power. The total efficiency of the laser was ~3.5 % and the slope efficiency was ~8.3 % (for the fourth component). The maximum power at $\lambda_{s4} = 2062$ nm (220 mW) is achieved at the 1472-nm pump power from the phosphosilicate converter equal to 6.25 W. The conversion efficiency is rather low because a considerable part of the pump power and of the first Stokes component is not absorbed. This is probably caused by a very large spectral width of the pump line (peak 3 in Fig. 8) and by the non-optimal choice of wavelengths for FBG writing: to obtain lasing at a wavelength above 2 μm after four-stage conversion, FBGs were written with the frequency shift considerably exceeding 427 cm^{-1}.

In fact, including the pump 1057-nm Yb-doped fibre laser, we used six-stage Raman laser to obtain lasing at 2 μm. This six-stage laser divided the optical frequency in half. However, because the efficiency of Raman lasers considerably decreases with increasing the number of stages [12], to reduce their number for producing efficient lasing at 2 μm and above, it is necessary to pump the Raman laser at wavelengths much greater than 1057 nm, which were used as in the scheme in Fig. 7.

5. Raman GeO_2 fibre lasers pumped by a 1.61-μm Er/Yb-doped fibre laser

By the reasons considered above, we used a 1608-nm Er/Yb-doped fibre laser (see, for example, [14]) with a two-element first cladding [7] for pumping. By employing this pump source, we fabricated the one-stage ($\lambda_{s1} = 1.73$ μm), two-stage ($\lambda_{s2} = 1851$ nm), three-stage ($\lambda_{s3} = 2027$ nm), and four-stage ($\lambda_{s4} = 2193$ nm) Raman fibre lasers.

The 1.73-μm one-stage laser was constructed using the scheme similar to that shown in Fig. 5, without the output FBG and without the FBG used for returning pump radiation. The efficiency of this laser was approximately the same as that of the 1571-nm Raman laser. By using this laser, we measured the value of $g_0(1.73/1.61)$.

The two-stage Raman laser was used as an intermediate laser for the development of the three-stage laser design. Its resonator was a GeO_2 fibre of length 60 m. The scheme of this laser was similar to that of the two-stage laser in Fig. 7

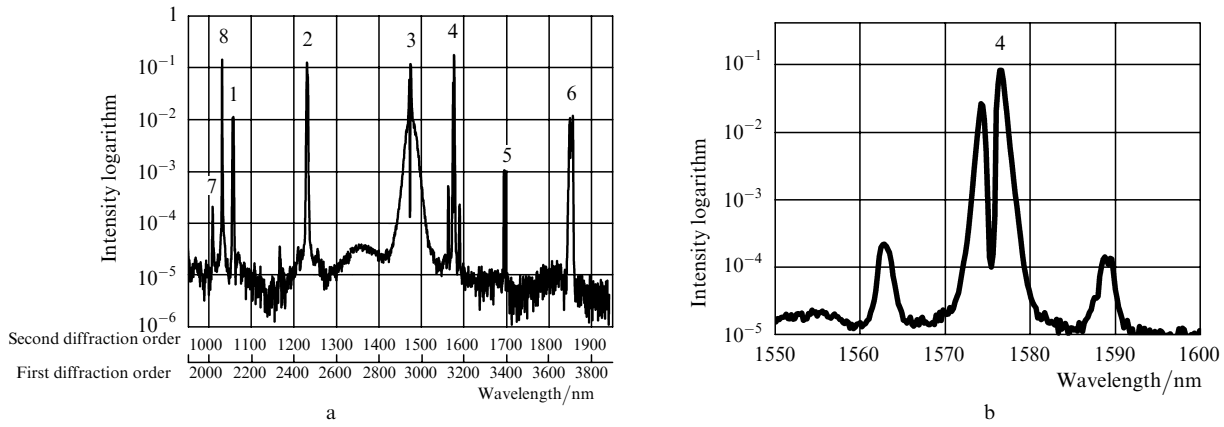

Figure 8. General emission spectrum of the composite multistage Raman fibre laser emitting 3.9 W in the 1472-nm line (peaks 1 – 6 are observed in the second diffraction order of the spectrometer, 7 and 8 – in the first diffraction order) (a) and the spectrum of the first 1576-nm Stokes component of the four-stage GeO_2 fibre laser; the side peaks shifted by ± 53 cm^{-1} and polarised in mutually perpendicular planes are distinctly observed (b). Peak 1 is the unabsorbed radiation of the 1.06-μm Yb laser; peak 2 is the 1231-nm radiation of the first stage of the phosphosilicate fibre laser; peak 3 is the 1472-nm radiation of the second stage of the phosphosilicate laser used to pump the four-stage GeO_2 fibre laser; peaks 4 – 6 correspond to the first (1575 nm), second (1695 nm), and third (1853 nm) Stokes components of the Raman GeO_2 fibre laser; peak 7 is the amplified SRS component of radiation with $\lambda_{s3} = 1853$ nm (without resonator) (2017 nm); and peak 8 is the 2062-nm fourth Stokes component of the Raman GeO_2 laser.

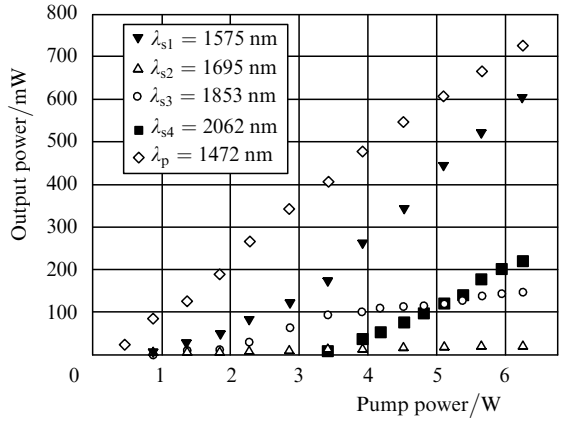

Figure 9. Dependences of the output power of the four Stokes components of the Raman GeO_2 fibre laser and the unabsorbed 1472-nm pump power on the pump power.

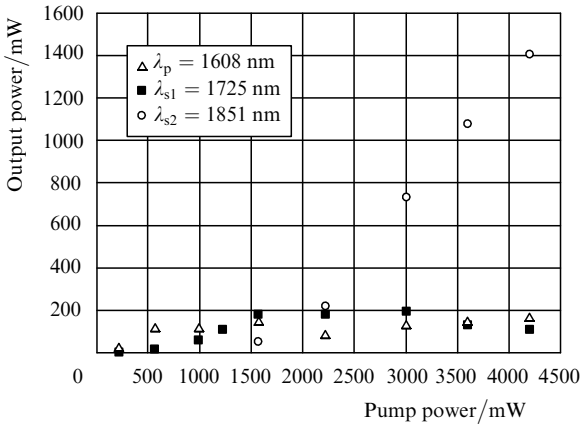

Figure 10. Dependences of the output power of Stokes components of the two-stage Raman laser on the 1608-nm pump power.

(with the resonance wavelengths of FBGs changed appropriately). The fibre end with the reflectivity ~ 3.5 % was used as the output mirror. We obtained lasing at 1851 nm at the maximum efficiency of 33 % (and the maximum slope efficiency of 60 %), and the output power achieved 1.4 W for the pump power of 4.2 W. The dependences of the power of different spectral components of the output radiation of the laser on the pump power are presented in Fig. 10. Note that the resonator length in this laser exceeded the optimal value.

The three-stage Raman fibre laser pumped at 1608 nm emitted at a wavelength above 2 μm. The laser design was optimised by simulating lasing numerically. The GeO_2 fibre length selected in this way was 13 m. Figure 11 shows the emission spectrum and dependences of the power of different spectral components of the laser on the pump power. Spectral lines 1, 2, 3, and 4 correspond to the 1608-nm pump radiation and the 1732-nm, 1864-nm, and 2027-nm radiation of the first, second, and third stages of the laser, respectively. The Stokes shifts between the radiation frequencies of the stages were chosen close to the corresponding frequencies of the maxima of the Raman gain of the fibre. The threshold pump power for lasing at the third stage was 1.6 W, while the maximum output power at 2027 nm achieved 900 mW for the pump power of 4.7 W, which corresponds to the total lasing efficiency of 19 %, the slope efficiency being 39 %.

In the development of the four-stage Raman GeO_2 fibre laser emitting at 2.2 μm, it is necessary to take into account a drastic increase in optical losses in the fibre in the spectral range from 2 to 2.2 μm. While optical losses in the three-stage laser at any of the wavelengths used do not exceed 40 dB km^{-1}, they amount to ~ 150 dB km^{-1} at 2.2 μm, which requires a considerable shortening of the fibre length (down to 8 m) and drastically reduces the laser efficiency (compared to that of the three-stage laser). We fabricated the four-stage Raman GeO_2 fibre laser emitting ~ 210 mW at 2193 nm at the pump power of 4.6 W. The total and slope efficiencies of the laser were 4.5 % and 6.2 %, respectively. The emission spectrum of the laser and the dependences of its output power on the pump power are shown in Fig. 12. Unfortunately, a considerable part of the pump power and

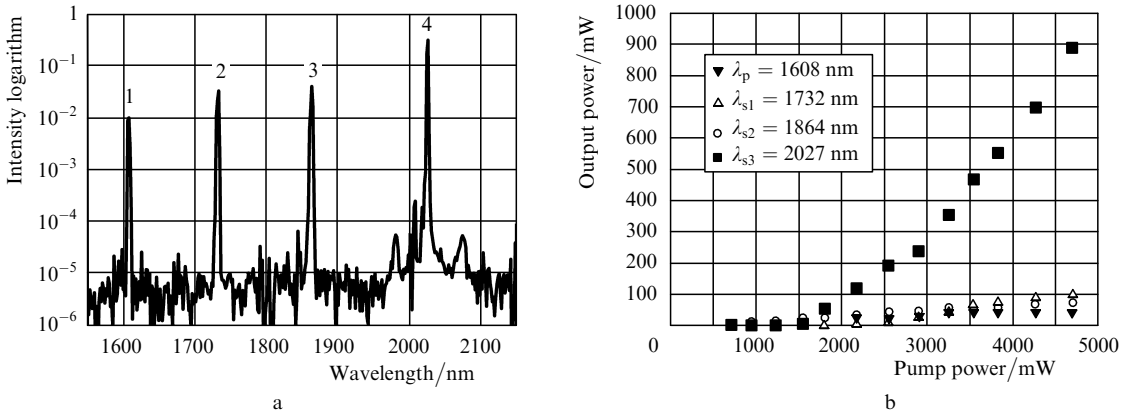

Figure 11. Output emission spectrum (a) and dependences of the power of Stokes components of the output radiation of the three-stage Raman laser on the pump power (b). Peak 1 is the unabsorbed 1608-nm pump radiation; peaks 2, 3, 4 correspond to radiation of the first ($\lambda_{s1} = 1732$ nm), second ($\lambda_{s2} = 1864$ nm), and third ($\lambda_{s3} = 2027$ nm) stages of the laser.

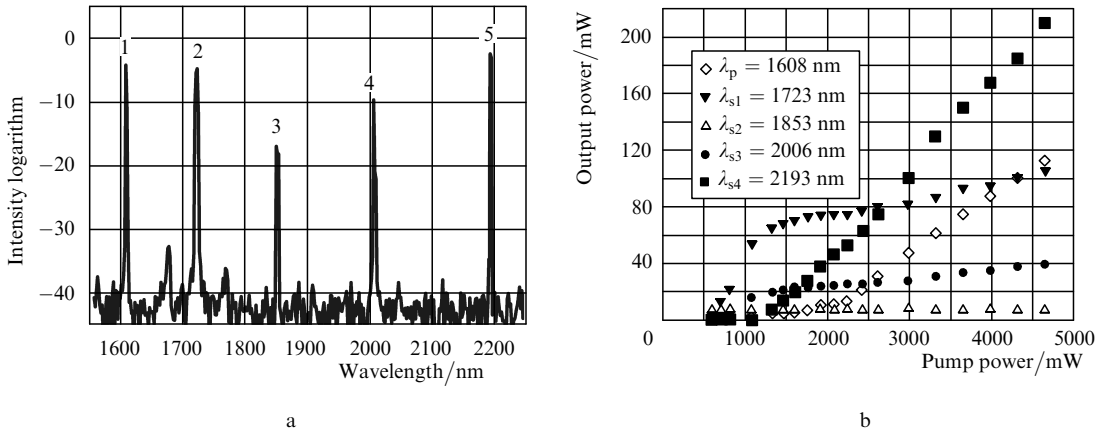

Figure 12. Output emission spectrum (a) and dependences of the power of Stokes components of the output radiation of the four-stage Raman laser on the pump power (b). Peak 1 is the unabsorbed 1608-nm pump radiation; peaks 2, 3, 4, 5 correspond to radiation of the first ($\lambda_{s1} = 1732$ nm), second ($\lambda_{s2} = 1853$ nm), third ($\lambda_{s3} = 2006$ nm), and fourth ($\lambda_{s4} = 2193$ nm) stages of the laser.

the first Stokes component is not absorbed in the laser.

Note that the wavelength of this Raman laser exceeds the wavelengths of all known silica fibre lasers, including thulium- and holmium-doped fibre lasers. The emission spectra of the two last lasers exhibit satellites of the lasing lines, similar to those shown in Fig. 8b: near the first Stokes component ($\lambda_{s1} = 1723$ nm) in the four-stage Raman laser (Fig. 12a) and near the last Stokes component ($\lambda_{s3} = 2027$ nm) in the three-stage laser (Fig. 11a). The fact that parametric processes in lasers of different design are manifested in different spectral regions can be associated with the use of GeO_2 fibres of different lengths in each Raman laser, whereas the parameters of the fibre (especially, dispersion parameters) could considerably change along its length.

6. Conclusions

The results obtained in the paper demonstrate the pronounced nonlinear properties of heavily GeO_2-doped fibres. Fibres of this type allowed a real breakthrough of Raman fibre lasers to the long-wavelength near-IR region – lasing at a wavelength of 2.2 μm was achieved and the emission region of Raman fibre lasers was broadened almost twice. A considerable increase in the Raman gain of the GeO_2 fibre with decreasing wavelength makes it possible to fabricate efficient fibre lasers emitting at ~1 μm despite the increase in optical losses. It seems that doping the fibre core with GeO_2 at even higher concentrations, if moderate optical losses are provided, will allow the fabrication of Raman lasers emitting in the spectral range from 2.5 to 3 μm.

References

1. Dianov E.M. *J. LightWave Tech.*, **20** (8), 1457 (2002).
2. Dianov E.M., Bufetov I.A., Mashinsky V.M., Neustruev V.B., Medvedkov O.I., Shubin A.V., Melkumov M.A., Gur'yanov A.N., Khopin V.F., Yashkov M.V. *Kvantovaya Elektron.*, **34**, 695 (2004) [*Quantum Electron.*, **34**, 695 (2004)].
3. Olshansky R., Sherer G.W. *Proc. 5th ECOC* (Amsterdam, 1979) Paper 12.5.1.
4. Dianov E.M., Mashinsky V.M., Neustruev V.B. *Kratk. Soobshch. Fiz. FIAN*, (3), 46 (1981).
5. Galeener F.L., Mikkelsen J.C., Geils R.H., Mosby W.J. *Appl. Phys. Lett.*, **32**, 34 (1978).
6. Mashinsky V.M., Neustruev V.B., Dvoyrin V.V., Vasiliev S.A., Medvedkov O.I., Bufetov I.A., Shubin A.V., Dianov E.M., Guryanov A.N., Khopin V.F., Salganskiy M.Yu. *Opt. Lett.*, **29**, 2596 (2004).

7. Bufetov I.A., Bubnov M.M., Melkumov M.A., Dudin V.V., Shubin A.V., Semenov S.L., Kravtsov K.S., Gur'yanov A.N., Yashkov M.V., Dianov E.M. *Kvantovaya Elektron.*, **35**, 328 (2005) [*Quantum Electron.*, **35**, 328 (2005)].
8. Bufetov I.A., Bubnov M.M., Larionov Y.V., Melkoumov M.A., Rybaltovsky A.A., Semjonov S.L., Dianov E.M., Vartapetov S.K., Obidin A.Z., Kurzanov M.A. *Proc. CLEO'2002* (Long Beach, 2002) CThJ5.
9. Dianov E.M., Bufetov I.A., Bubnov M.M., Grekov M.V., Shubin A.V., Vasil'ev S.A., V.M., Medvedkov O.I., Semenov S.L., Egorova M.N., Gur'yanov A.N., Khopin V.F., Yashkov M.V., Varelas D., Iokko A., Kostantini D., Limberger N.G., Salate R.-P. *Kvantovaya Elektron.*, **29**, 97 (1999) [*Quantum Electron.*, **29**, 935 (1999)].
10. Dianov E.M., Bufetov I.A., Bubnov M.M., Grekov M.V., Vasiliev S.A., Medvedkov O.I., Shubin A.V., Guryanov A.N., Khopin V.F., Yashkov M.V., DeLiso E.M., Butler D.L. *Proc. SPIE Int. Soc. Opt. Eng.*, **4083**, 101 (2000).
11. Stolen R.H. *Optical Fiber Telecommunication* (New York: Acad. Press, 1979) pp 125–150.
12. Bufetov I.A., Dianov E.M. *Kvantovaya Elektron.*, **30**, 873 (2000) [*Quantum Electron.*, **30**, 873 (2000)].
13. Agraval G. *Nonlinear Fibre Optics* (Boston: Academic Press, 2001; Moscow: Mir, 1996).
14. Cheo P.K., King G.G. *IEEE Photon. Technol. Lett.*, **13**, 188 (2001).